# Photon paths in the hyperbolic topological black hole spacetime of conformal Weyl gravity

## Graeme Candlish<sup>a</sup> Marco Olivares<sup>b</sup> Constanza Osses<sup>c</sup> J. R. Villanueva<sup>a</sup>

E-mail: graeme.candlish@uv.cl, marco.olivaresr@mail.udp.cl, constanza.osses.g@mail.pucv.cl, jose.villanueva@uv.cl

**Abstract.** In this work we find analytical solutions to the null geodesics in the hyperbolic topological black hole spacetime of conformal Weyl gravity in an invariant 2-plane given by the orbits of an azimuthal Killing vector. Exact expressions for the (non-compact) horizons are found, which depend on the cosmological constant and the coupling constants of conformal Weyl gravity. The angular motion is examined qualitatively by means of an effective potential; quantitatively, the equation of motion is solved in terms of the  $\wp$ -Weierstraß elliptic function. Thus, we find the deflection angle for photons without using any approximation, which is a novel result for this topology.

Keywords: Modified Gravity; Black Holes; Elliptic Functions.

<sup>&</sup>lt;sup>a</sup> Instituto de Física y Astronomía, Universidad de Valparaíso, Avenida Gran Bretaña 1111, Casilla 5030, Playa Ancha, Valparaíso, Chile

<sup>&</sup>lt;sup>b</sup>Facultad de Ingeniería y Ciencias, Universidad Diego Portales, Avenida Ejército Libertador 441, Casilla 298-V, Santiago, Chile.

<sup>&</sup>lt;sup>c</sup>Instituto de Física, Pontificia Universidad Católica de Valparaíso, Avenida Universidad 330, Curauma, Valparaíso, Chile

 $<sup>^{1}</sup>$ Corresponding author.

#### Contents

1	Introduction: Conformal Weyl gravity and null geodesics	1
2	Hyperbolic topological black hole spacetime in conformal Weyl gravity 2.1 Allowed orbits 2.2 Bending of light	<b>2</b> 6 8
3	Summary	9

### 1 Introduction: Conformal Weyl gravity and null geodesics

Conformal Weyl gravity (CWG) [1–4] corresponds to a fourth order theory in which the spacetime geometry is invariant under the local change

$$g_{\mu\nu}(x) \to \Omega^2(x) g_{\mu\nu}(x),$$
 (1.1)

where  $\Omega(x)$  is any smooth strictly positive function. The restrictive conformal invariance then leads to the unique action

$$I_W = -\alpha \int d^4x \sqrt{-g} C_{\lambda\mu\nu\kappa} C^{\lambda\mu\nu\kappa} = -2\alpha \int d^4x \sqrt{-g} \left[ R_{\mu\kappa} R^{\mu\kappa} - \frac{1}{3} R^2 \right], \qquad (1.2)$$

where  $\alpha$  is the dimensionless gravitational coupling constant, and  $C_{\lambda\mu\nu\kappa}$  is the conformal Weyl tensor given by

$$C_{\lambda\mu\nu\kappa} = R_{\lambda\mu\nu\kappa} - \frac{1}{2}(g_{\lambda\nu}R_{\mu\kappa} - g_{\lambda\kappa}R_{\mu\nu} - g_{\mu\nu}R_{\lambda\kappa} + g_{\mu\kappa}R_{\lambda\nu}) + \frac{1}{6}R(g_{\lambda\nu}g_{\mu\kappa} - g_{\lambda\kappa}g_{\mu\nu}). \quad (1.3)$$

Note that the action (1.2) naturally appears as the difference between a Weyl-squared term and the Gauss-Bonnet invariant in 3+1 dimensions. Although the Gauss-Bonnet term is a topological invariant in that case, its addition is far from trivial, since one can prove that this is equivalent to the renormalization program in the context of AdS / CFT [5].

The gravitational field equations associated to the action (1.2) are given by

$$\sqrt{-g} g_{\mu\alpha} g_{\nu\beta} \frac{\delta I_W}{\delta g_{\alpha\beta}} = -2 \alpha W_{\mu\nu} = -\frac{1}{2} T_{\mu\nu}, \qquad (1.4)$$

where  $T_{\mu\nu}$  is the stress-energy tensor, and  $W_{\mu\nu}$  is the Bach tensor given by

$$W_{\mu\nu} = 2C^{\alpha\beta}_{\mu\nu;\beta\alpha} + C^{\alpha\beta}_{\mu\nu} R_{\alpha\beta}. \tag{1.5}$$

An exact vacuum solution to the field equations (1.4) is given, up to a conformal factor and in the usual Schwarzschild coordinates  $(\tilde{t}, \tilde{r}, \Theta, \Phi)$ , by the static spherically symmetric metric [6–10]

$$d\tilde{s}^2 = -B(\tilde{r}) d\tilde{t}^2 + \frac{d\tilde{r}^2}{B(\tilde{r})} + \tilde{r}^2 d\Omega^2, \tag{1.6}$$

where  $d\Omega^2 = d\Theta^2 + \sin^2\Theta d\Phi^2$  is the standard metric on the 2–sphere, and the lapse function is

$$B(\tilde{r}) = 1 - \frac{(2 - 3M\tilde{\gamma})M}{\tilde{r}} - 3M\tilde{\gamma} + \tilde{\gamma}\tilde{r} - k\tilde{r}^2.$$

$$(1.7)$$

Here M is the central mass,  $k = \Lambda/3$  is the cosmological constant and  $\tilde{\gamma}$  is the Weyl parameter, which can be related to the interior dynamics of the static source of interest and the properties of the background geometry. A great deal of investigation has taken place in conformal gravity. For example, the treatment of bending of light from various points of view can be found in [11–18], while the gravitomagnetic and Sagnac effects are investiged in [19] and [20], respectively. Black hole solutions with other properties such as electric charge, angular momentum and non-trivial topology are found in [21–25], and also a general class of wormhole geometries in CWG is analyzed in [26]. On the other hand, some cosmological implications have been studied in the literature, see for example [27–31], whereas some studies investigating finite mass distributions such as stars may be found in [32, 33]. An study of the motion of massless particles in the exterior space-time of a toroidal topological black hole can be found in [34].

Study of the motion of test particles can be obtained using the standard Lagrange procedure [35–43], which makes it possible to associate a Lagrangian  $\mathcal{L}$  with the metric and then obtain the equation of motion from Lagrange's equations

$$\dot{\Pi}_q - \frac{\partial \mathcal{L}}{\partial q} = 0, \tag{1.8}$$

where  $\Pi_q = \partial \mathcal{L}/\partial \dot{q}$  are the conjugate momenta to the coordinate q, and the dot denotes a derivative with respect to the affine parameter  $\tau$  along the geodesic. In the next sections, following the procedure performed by Klemm [22] and taking into account that the metric (1.6), we perform an analytical continuation to obtain a non-trivial topology associated with black holes in CWG, and then we study the null geodesics on these manifolds.

Finally, as we can see from the metric (1.6)–(1.7), in this work we will use geometrized units (G=1 and c=1), so the parameters have the typical values  $k \approx 4.1 \times 10^{-20} \, pc^{-2}$  and  $\tilde{\gamma} \approx 3.1 \times 10^{-10} \, pc^{-1}$ .

#### 2 Hyperbolic topological black hole spacetime in conformal Weyl gravity

In order to obtain a class of topological black hole solutions, we perform the analytical continuation suggested by [22]:

$$d\tilde{s} \to \frac{ds}{M}, k \to M^2 k, \tilde{\gamma} \to i M \gamma, M \to \frac{-i}{M}, \tilde{t} \to \frac{i t}{M}, \tilde{r} \to \frac{i r}{M}, \Phi \to \phi, \Theta \to i \theta,$$
 (2.1)

so Eqs. (1.6)–(1.7) yield to

$$ds^{2} = -B(r) dt^{2} + \frac{dr^{2}}{B(r)} + r^{2} (d\theta^{2} + \sinh^{2}\theta d\phi^{2}),$$
 (2.2)

$$B(r) = -1 - \frac{(2 - 3\gamma)}{r} + 3\gamma + \gamma r - kr^2, \tag{2.3}$$

and the Lagrangian reads

$$\mathcal{L} = \frac{1}{2}B(r)\dot{t}^2 + \frac{\dot{r}^2}{2B(r)} + \frac{r^2}{2}(\dot{\theta}^2 + \sinh^2\theta \,\dot{\phi}^2). \tag{2.4}$$

Clearly, the metric induced on the spacelike surface of constants t and r is the standard metric of hyperbolic 2-space  $\mathbb{H}^2$ ,  $d\sigma^2 = r^2(d\theta^2 + \sinh^2\theta \, d\phi^2)$ , which has a constant negative curvature and is not compact. In [22] the  $(\theta, \phi)$ -sector is compactified by acting with an appropriate discrete subgroup G of the isometry group SO(2;1) of  $\mathbb{H}^2$ , to form the compact quotient space  $\mathbb{H}^2/G$ . Upon demanding an orientable manifold, this space becomes a Riemann surface  $S_g$  of genus g > 1, and the topology of the four-dimensional manifold is  $\mathbb{R}^2 \times S_g$  (the details of the compactification procedure are given in [44]). In this work we will not apply this compactification procedure, but will instead consider the non-compact hyperbolic 2-space  $\mathbb{H}^2$ . The spatial slices of the event horizon in this solution are therefore non-compact hyperbolic spaces, and the solution may be considered an exotic type of black membrane.

As discussed in [22], additional parameter choices may be made to construct black hole spacetimes with non-trivial topology: i) Setting  $\gamma=0$  and  $k=\Lambda/3<0$ , where  $\Lambda$  is the cosmological constant, one recovers the uncharged, static topological black hole solutions in AdS gravity. ii) We may set k=0, yielding a solution which is not asymptotically AdS. iii) For k>0,  $\gamma>0$  and  $\gamma_e<\gamma<2/3$  the spacetime has a black hole interpretation,  $\gamma=\gamma_e$  yielding an extreme black hole, where  $\gamma_e^2(1-\gamma_e)/(2-3\gamma_e)^2=k$ . On the other hand, it is not hard to show that the scalar curvature R diverges at r=0 so we have a curvature singularity at the origin. In addition, R vanishes for  $r\to\infty$  if k=0, although the manifold is not Ricci-flat at infinity and therefore is not asymptotically Minkowski space. For this value of k the manifold is globally hyperbolic, which is not the case for AdS black holes, see [22].

From the hyperbolic lapse function (2.3), it is possible to construct the cubic polynomial

$$p_3(r) = -\frac{rB(r)}{k} = r^3 - \frac{\gamma}{k}r^2 + \frac{(1-3\gamma)}{k}r + \frac{(2-3\gamma)}{k},\tag{2.5}$$

which gives us the locations of the horizons (if there are any). In fact, defining  $r_w = \gamma/3k$  and then making the change of variable:

$$r = x + r_w, (2.6)$$

we write the cubic polynomial in its canonical form

$$p_3(x) = x^3 - \eta_2 x - \eta_3, (2.7)$$

where the coefficients are given by

$$\eta_2 = 3r_w^2 + 9r_w - \frac{1}{k},\tag{2.8}$$

$$\eta_3 = 2r_w^3 + 9r_w^2 + \left(9 - \frac{1}{k}\right)r_w - \frac{2}{k}.$$
 (2.9)

Obviously, the nature of the coefficients depends on the combination of the pair  $(\gamma, k)$ . In Fig. 1 three different regions appear with the possible choice of the sign of  $\eta_2$  and  $\eta_3$  on the k- $\gamma$  plane. In the region between  $\gamma = 0$  and  $\eta_2 = 0$ , the roots of the polynomial  $p_3(x)$  satisfy the equation  $x^3 + |\eta_2|x + |\eta_3| = 0$ , so there is no real solution for x > 0, and thus we dismiss this case. On the other hand, one may obtain information about the roots from the cubic discriminant  $\Delta_c = 27\eta_3^2 - 4\eta_2^3$ . Thus, if  $\Delta_c < 0$ , there is one real negative root and a complex pair of roots, representing a naked singularity; if  $\Delta_c > 0$ , there are three different real roots, two positive and one negative, which looks similar to the SdS spacetime with an event and cosmological horizons. Finally, if  $\Delta_c = 0$ , there are three real roots, one

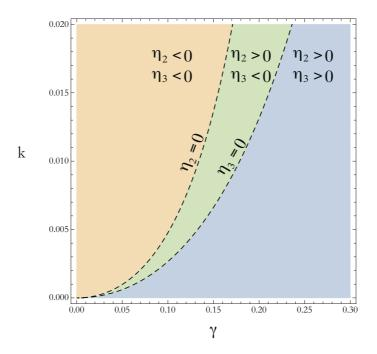


**Figure 1.** This region plot shows the sign of the cubic parameters of the polynomial (2.7),  $\eta_2$  and  $\eta_3$ , on the k- $\gamma$  plane. The region in which  $\eta_2 < 0$  and  $\eta_3 < 0$  does not allow a real solution to the equation  $p_3(x) = 0$ .

negative and a degenerate positive root, representing the extreme case. Thus, for example, if we assume that  $\gamma$  is small, then the coefficient  $\eta_3$  is negative, and therefore the discriminant of the polynomial is positive,  $\Delta_c > 0$ .

Denoting

$$R = \sqrt{\frac{|\eta_2|}{3}}, \quad \varphi = \frac{1}{3}\arccos\left(\frac{\eta_3}{R^3}\right),$$
 (2.10)

we can find the expression for the event horizon,  $r_+$ , the cosmological horizon,  $r_{++}$ , and the negative root (without physical meaning),  $r_n$ . They take the form

$$r_{+} = r_{w} + \frac{R}{2}(\cos\varphi - \sqrt{3}\sin\varphi), \qquad (2.11)$$

$$r_{++} = r_w + R\cos\varphi,\tag{2.12}$$

$$r_n = r_w - \frac{R}{2}(\cos\varphi + \sqrt{3}\sin\varphi). \tag{2.13}$$

Conversely, the (non-compact) hyperbolic metric (2.2) admits the following Killing vector fields [45]:

• the time-like Killing vector  $\xi = \partial_t$  is related to the stationarity of the metric. The conserved quantity is given by

$$g_{\mu\nu}\,\xi^{\mu}\,u^{\nu} = -B(r)\,\dot{t} = -\sqrt{E}$$
 (2.14)

where E is a constant of the motion that cannot be associated with the total energy of the test particle because this metric is not asymptotically flat.

• the most general space-like Killing vector is given by

$$\vec{\xi} = (A\cos\phi + B\sin\phi) \ \partial_{\theta} + [C - \coth\theta \ (A\cos\phi + B\sin\phi)] \ \partial_{\phi}, \tag{2.15}$$

where A, B and C are arbitrary constants. It is easy to see that this is a linear combination of the three Killing vectors

$$\chi_1 = \partial_{\phi}, \quad \chi_2 = -\coth\theta \sin\phi \,\partial_{\phi} + \cos\phi \,\partial_{\theta}, \quad \chi_3 = \coth\theta \cos\phi \,\partial_{\phi} + \sin\phi \,\partial_{\theta},$$

which are the angular momentum operators for this spacetime. The conserved quantities are given by

$$g_{\alpha\beta} \chi_1^{\alpha} u^{\beta} = r^2 \sinh^2 \theta \,\dot{\phi} = L_1,\tag{2.16}$$

$$g_{\alpha\beta} \chi_2^{\alpha} u^{\beta} = r^2 (\cos \phi \,\dot{\theta} - \sinh \theta \,\cosh \theta \sin \phi \,\dot{\phi}) = L_2, \tag{2.17}$$

$$g_{\alpha\beta} \chi_3^{\alpha} u^{\beta} = r^2 (\sin \phi \,\dot{\theta} + \sinh \theta \, \cosh \theta \, \cos \phi \,\dot{\phi}) = L_3, \tag{2.18}$$

where  $L_1$ ,  $L_2$  and  $L_3$  are constants associated with the angular momentum of the particles. Thus, from Eqs. (2.16–2.18), it is easy to demonstrate that

$$\frac{J^2}{r^4} \equiv \frac{(L_2^2 + L_3^2) - L_1^2}{r^4} = \dot{\theta}^2 + \sinh^2 \theta \dot{\phi}^2. \tag{2.19}$$

We now focus our attention, without loss of generality, on the invariant 2-plane  $\theta = \arcsin(1)$ , so  $\dot{\theta} = 0$ , and therefore Eq. (2.19) reduces to

$$\dot{\phi} = \frac{J}{r^2}.\tag{2.20}$$

Using Eqs. (2.14) and (2.20), and taking into account that the Lagrangian associated with the motion of photons is null,  $\mathcal{L} = 0$ , it is easy to obtain the radial equation of motion

$$\dot{r}^2 = E - V(r),\tag{2.21}$$

where V(r) is the effective potential which satisfies the relation

$$\frac{V(r)}{E} \equiv \mathcal{V}(r) = b^2 \frac{B(r)}{r^2},\tag{2.22}$$

and  $b=J/\sqrt{E}$  is the impact parameter. This last point is relevant for the radial motion, since  $V(r) \propto b^2 = 0$ ; the familiar and well studied relation  $\dot{r} = \pm \sqrt{E}$  is recovered. In its essence, the motion presents the same features known in other spacetimes (see for example [35–37]). On the other hand, by combining Eqs. (2.20) and (2.21), we obtain the radial–polar equation

$$\left(\frac{dr}{d\phi}\right)^2 = \frac{r^4}{b^2} \left[1 - \mathcal{V}(r)\right]. \tag{2.23}$$

In Fig.2 we have plotted the conformal effective potential (per unit of  $b^2$ ) as a function of the radial coordinate, for a fixed value of the cosmological parameter k = 0.05. The evolution of the curves was made in terms of the Weyl parameter  $\gamma$ . Thus, as with Einstein's black hole, the position of the maximum  $r_m$  is independent of k and is thus only a function of  $\gamma$ :

$$r_m = 3\left(\frac{\gamma_c}{\gamma} - 1\right),\tag{2.24}$$

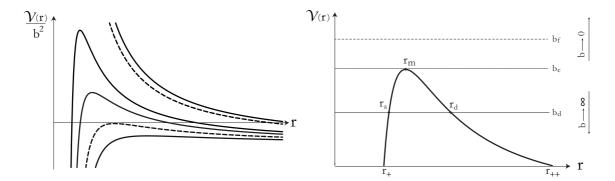


Figure 2. Left panel: Evolution of the conformal effective potential, per unit of  $b^2$ , for photons in Weyl's gravity as a function of the Weyl parameter  $\gamma$  with a fixed value of the cosmological parameter k=0.05. The upper dashed line corresponds to the curve with  $\gamma=\gamma_c$  while the lower dashed line corresponds to the extreme topological black hole, for which the relation  $V_m=0$  is satisfied. Right panel: Typical effective potential with three general regions for the motion of photons: deflection zone, in which the impact parameter poses a value between  $[b_c < b \equiv b_d < \infty]$ , asymptotic zone, in which the impact parameter has the value  $b=b_c$ , and a capture zone in which the impact parameter has a value between  $[0 < b \equiv b_f < b_c]$ .

where  $\gamma_c = 2/3$ . At this point the impact parameter assumes the critical value

$$b_c = \frac{1}{\sqrt{k_{ext} - k}},\tag{2.25}$$

where  $k_{ext} = (1 - \gamma)/r_m^2$ . In the same figure, the upper dashed line represents the effective potential for  $\gamma_c$ , which implies that  $r_m = 0$  and  $V(r_m) \equiv V_m \to \infty$ , whereas on the lower dashed line the relation  $k = k_{ext}$  is satisfied, which represents the extreme case for which  $V_m = 0$ . Note that the latter condition implies that  $b_c \to \infty$ . With this in mind, we focus our attention on the family of potentials that lie between these two well defined curves. The next subsection is devoted to analyzing the effective potential qualitatively in terms of the impact parameter.

#### 2.1 Allowed orbits

As we have mentioned, under the assumption that  $\gamma < \gamma_c$  and  $k < k_{ext}$ , massless particles can perform different kinds of orbits, which depend on their impact parameter. In this way, based on the classification of b shown in the left panel of Figure 2, we present a brief qualitative description of the angular motions permitted for photons in the chosen invariant 2-plane of the non-compact hyperbolic topological black hole spacetimes in conformal Weyl gravity.

• Unbounded trajectories (capture zone): If  $0 < b \equiv b_f < b_c$ , the incident photons fall inexorably to one of the two horizons, depending on the initial conditions placed on their velocity. The cross section,  $\sigma$ , in this geometry is [43]

$$\sigma = \pi b_c^2 = \frac{\pi}{k_{ext} - k}.$$
 (2.26)

• Critical trajectories: If  $b = b_c$ , photons can stay in the unstable inner circular orbit of radius  $r_m$ . Therefore, the photons that arrive from the initial distance  $r_i$  ( $r_+ < r_i < r_m$ ,

or  $r_m < r_i < r_{++}$ ) can asymptotically fall to a circle of radius  $r_m$ . The proper period in such an orbit is given by

$$T_{\tau} = \frac{2\pi r_m^2}{J} = \frac{18\pi}{J} \left(\frac{\gamma_c}{\gamma} - 1\right)^2,$$
 (2.27)

which is independent of k, whereas the coordinate period depends on k and  $\gamma$  as

$$T_t = 2\pi b_c = \frac{2\pi}{\sqrt{k_{ext} - k}}. (2.28)$$

• Deflection Zone. If  $b_c < b = b_d < \infty$ , the photons come from a finite distance  $r_i$   $(r_+ < r_i < r_m$  for orbits of the first kind or  $r_m < r_i < r_{++}$  for orbits of the second kind) to a turning point  $r_t$  (which is the solution to the equation  $\mathcal{V}(r_t) = 1$ ), and then return to one of the two horizons. Therefore, by defining

$$R_W = \frac{\gamma \mathcal{B}^2}{3}, \quad \bar{R} = \sqrt{\frac{\varrho_2}{3}}, \quad \zeta = \frac{1}{3}\arccos\sqrt{\frac{27\varrho_3^2}{\varrho_3^2}},$$
 (2.29)

where the cubic coefficients are given by

$$\varrho_2 = 3 \gamma_c^2 \mathcal{B}^2 \left[ \gamma^2 \mathcal{B}^2 + 3 \left( \frac{3 - r_m}{3 + r_m} \right) \right],$$
(2.30)

and

$$\varrho_3 = \gamma_c^2 \,\mathcal{B}^2 \left[ \gamma_c \,\gamma^3 \,\mathcal{B}^4 + \frac{6(3 - r_m)}{(3 + r_m)^2} \,\mathcal{B}^2 - \frac{18 \,r_m}{3 + r_m} \right],\tag{2.31}$$

and  $\mathcal{B}$  is the anomalous impact parameter given by

$$\mathcal{B} = \frac{b}{\sqrt{1+k\,b^2}},\tag{2.32}$$

these solutions are given explicitly through the following equations:

$$r_1 = R_W - \frac{R}{2} \left( \sqrt{3} \sin \zeta + \cos \zeta \right), \tag{2.33}$$

$$r_a = R_W + \frac{R}{2} \left( \sqrt{3} \sin \zeta - \cos \zeta \right), \tag{2.34}$$

$$r_d = R_W + \bar{R}\cos\zeta. \tag{2.35}$$

Notice that if the condition  $\varrho_2^3 > 27\varrho_3^2$  is assumed, it is not difficult to show that the preceding solutions satisfy  $r_1 < 0 < r_a < r_d$ . Also note that, as has been pointed out by Cruz et al. [36], since k is very small, only when  $b \sim k^{-1/2}$  is the net effect of  $\mathcal B$  relevant in (2.32). Also, if the product  $k b^2 \gg 1$  (or  $b \to \infty$ ), then  $\mathcal B \sim k^{-1/2}$  in such a way that  $\varrho_2 \to \eta_2$  and  $\varrho_3 \to \eta_3$  (cf. Eqs. (2.8)–(2.30) and Eqs. (2.9)–(2.31)). Therefore, as expected, the identities  $r_a(\infty, \gamma, k) = r_+$  and  $r_d(\infty, \gamma, k) = r_+$  can be proven in a few steps [17].

In order to obtain the analytical expression for the orbit in which the photons are moving, we perform an integration of Eq. (2.23), resulting in

$$r(\phi) = |x_1| \pm \frac{1}{4\wp(\kappa \phi; g_2, g_3) - \alpha_1/3}, \quad \text{if} \quad b_c < b < \infty,$$

$$r(\phi) = \frac{1}{4\wp(\kappa \phi + \omega_0; g_2, g_3) - \alpha_1/3}, \quad \text{if} \quad 0 < b \le b_c,$$
(2.36)

$$r(\phi) = \frac{1}{4\wp(\kappa \phi + \omega_0; q_2, q_3) - \alpha_1/3}, \quad \text{if} \quad 0 < b \le b_c,$$
 (2.37)

where  $\wp(x; g_2, g_3)$  is the  $\wp$ -Weierstraß elliptic function, whose Weierstraß invariants are given by

$$g_2 = \frac{1}{4} \left( \frac{\alpha_1^2}{3} - \beta_1^2 \right), \qquad g_3 = \frac{1}{16} \left( \frac{\alpha_1 \beta_1^2}{3} - \frac{2}{27} \alpha_1^3 - \gamma_1^3 \right),$$
 (2.38)

whereas the constants appearing in Eqs. (2.36-2.38) are given explicitly by

$$\kappa = \frac{\sqrt{x_1 \, x_2 \, x_3}}{\mathcal{B}}, \qquad \alpha_1 = \frac{1}{x_1} + \frac{1}{x_2} + \frac{1}{x_3}$$
$$\beta_1 = \left[\frac{1}{x_1 \, x_2} + \frac{1}{x_1 \, x_3} + \frac{1}{x_2 \, x_3}\right]^{1/2}, \qquad \gamma_1 = \frac{1}{[x_1 \, x_2 \, x_3]^{1/3}}.$$

Also, the plus and minus sign in Eq. (2.36) correspond to orbits of the first kind  $(r \geq r_d)$ and orbits of the second kind  $(r \leq r_a)$ , respectively (see right panel of Fig. 2), and the values of  $x_i$  (j=1,2,3) depend on the region where the motion occurs as well as the type of orbit. Table 2.1 summarizes the values used in Equations (2.36) and (2.37), which depend on the value of the impact parameter, whereas in Fig. 3 the trajectories obtained from Equation (2.37) are shown, i.e., for photons with  $b \leq b_c$ .

**Table 1.** Quantities used in Eqs. (2.36) and (2.37) to obtain the trajectories of the photons in the exterior geometry of a non-compact hyperbolic topological black hole spacetime in conformal Weyl gravity.

 · 10.5.										
Type of orbit	Range for $r$	Range for $b$	$x_1$	$x_2$	$x_3$	ω				
First kind	$r > r_d$	$b_c < b < \infty$	$r_d$	$r_d - r_a$	$r_d - r_1$					
Second kind	$r < r_a$	$b_c < b < \infty$	$-r_a$	$r_d - r_a$	$-(r_a-r_1)$					
$Critical\ FK$	$r > r_m$	$b = b_c$	$r_1$	$-r_d$	$-r_a$	$\wp^{-1}(\frac{\alpha_1}{12})$				
$Critical\ SK$	$r < r_m$	$b = b_c$	$r_1$	$-r_d$	$-r_a$	0				
Unbounded	$r > r_+$	$0 < b < b_c$	$r_1$	$-r_d$	$-r_a$	0				

#### 2.2Bending of light

As an application of the preceding section, specifically of the polar equation (2.36) for the photon orbit of the first kind, it is possible to study how this is deflected due to presence of the non-compact black hole, whose singularity, for the sake of simplicity, is placed at the origin of a coordinate system O. Therefore, in order to obtain a full description, we employ the exact method outlined by Villanueva & Olivares [17] instead of the Rindler-Ishak method performed in other works [14, 18, 46–48].

Suppose that in  $t = t_0$  photons are emitted with impact parameter  $b_c < b < \infty$  by a source placed at  $(r_i, \theta_i) = (r_{\bigstar}, \theta_{\bigstar})$  with respect to O. Therefore, photons travelling in the

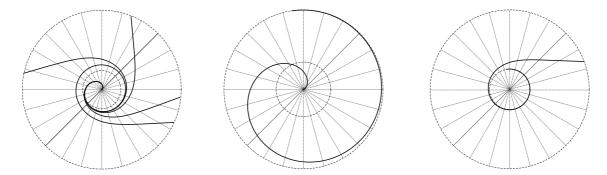


Figure 3. Plots referring to Eq. (2.36) in a cut of the  $\phi=\pi/2$ -invariant plane of the non-compact hyperbolic topological Weyl black hole spacetime. LEFT PANEL: Unbounded trajectory for massless particles with  $b < b_c$ . The fall to the cosmological horizon or event horizon depends on the initial direction of their motion. MIDDLE PANEL: Critical trajectory of the first kind, in which  $r_i < r_m$  and  $b = b_c$ . Photons can asymptotically fall to a circle of radius  $r_m$  or fall to the event horizon. RIGHT PANEL: Critical trajectory of the second kind, in which  $r_i > r_m$  and  $b = b_c$ . Photons can asymptotically fall to a circle of radius  $r_m$  or fall to the cosmological horizon.

exterior spacetime of the non-compact hyperbolic topological black hole are deflected in such way they reach the turning point  $r_d$  given by Eq. (2.34), and then are received by an observer placed at the position  $(r_{\bigoplus}, -\theta_{\bigoplus})$  on the manifold (see left-top panel of Fig. 4). Based on the same plot, it is not difficult to prove that

$$\widehat{\alpha} = |\theta_{\star}| + |\theta_{\oplus}| - \pi; \tag{2.39}$$

therefore, by combining Eq. (2.36) with Eq. (2.39), the deflection angle becomes

$$\widehat{\alpha} = \frac{1}{\kappa} \left( \left| \wp^{-1} \left[ \frac{1}{4(r_{\bigstar} - r_d)} + \frac{\alpha_1}{12} \right] \right| + \left| \wp^{-1} \left[ \frac{1}{4(r_{\bigoplus} - r_d)} + \frac{\alpha_1}{12} \right] \right| \right) - \pi, \tag{2.40}$$

where  $\wp^{-1}$  is the inverse  $\wp$ -Weierstraß function [49–52]. In the bottom left panel of Fig. 4, the deflection angle as a function of  $b^{-2}$  is plotted, and it shows that there is a special value at which the deflection angle vanishes. This means that the scattering of photons by a hyperbolic topological black hole can be attractive or repulsive (with respect to the black hole), depending on the influence of the event horizon or the cosmological horizon (see top and bottom right panel of Fig. 4).

#### 3 Summary

In this research, we have studied the null geodesics of a non-compact hyperbolic topological black hole spacetime in conformal Weyl gravity, the metric of which is given by Eq. (2.3). In this context, we analyze the existence of the event horizon,  $r_+$ , and the cosmological horizon,  $r_{++}$ , as a function of the cosmological parameter k, and the Weyl parameter,  $\gamma$ , as shown in Fig. 1, and we obtain their analytical expression in terms of these parameters. Also, the Killing vector fields are obtained and the associated four conserved quantities, showing the stationarity and the rotational invariance of the metric. These symmetries reduce our study to a unidimensional equivalent problem on an invariant plane, which is chosen to be  $\phi = \pi/2$ . A quick view of the equations of motion show us that the radial motion of photons presents the same features performed in the standard conformal Weyl gravity [17], and therefore, in

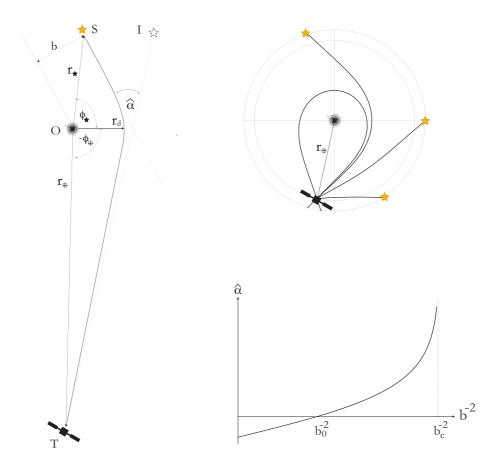


Figure 4. Gravitational lensing from a non-compact hyperbolic topological black hole in conformal Weyl gravity. LEFT: Light with impact parameter b from the source S at  $(r_{\bigstar}, \theta_{\bigstar})$  bends at the lens O and arrives at the observer T at  $(r_{\oplus}, -\theta_{\oplus})$ , who then sees the image I; TOP RIGHT: Trajectories for different values of the impact parameter as observed at T; BOTTOM RIGHT: The angle of deflection  $\widehat{\alpha}$  as a function of  $b^{-2}$ . There is a critical value of the impact parameter  $b_0$ , for which the deflection angle vanishes and thus the bending of light can be attractive or repulsive. Also, the deflection angle approaches infinity as the impact parameter approaches the critical value  $b_c$ .

the same way as Einstein's black holes, photons cross the horizons in a finite proper time, whereas in an external system, the photons fall asymptotically to the horizons.

The angular motion was first studied qualitatively by means of an analysis of the effective potential as a function of the radial distance for different values of the impact parameter b (see Fig. 2). Therefore, under the condition  $\gamma < \gamma_c$  and  $k < k_{ext}$ , this analysis shows the existence of a maximum for which photons with  $b = b_c = (k_{ext} - k)^{-1/2}$  either fall to one of the horizons or tend asymptotically to an unstable circular orbit at  $r_m$ . Also, we note that the existence of the unstable circular orbit depends on the parameter  $\gamma$ , which is a novel result because in the standard conformal Weyl gravity this only depends on the mass M [17]. For this reason, the proper period also depends on the Weyl parameter  $\gamma$ , whereas the coordinate period, as we expect, depends on  $\gamma$  and k. However, if the value of the impact parameter is  $0 < b < b_c$ , then photons fall inexorably to one of the horizons. Finally, when the impact parameter is  $b = b_d$  so  $b_c < b_d < \infty$ , the trajectory is deflected in such a way that for  $r \le r_a$  then  $r_a$  corresponds to an apoastron distance, or for  $r \ge r_d$  the distance

 $r_d$  corresponds to a periastron distance. The exact calculation of both distances,  $r_a$  and  $r_d$ , makes it possible to verify that in the limit  $b \to \infty$ , the consistency relations  $r_a \to r_+$  and  $r_d \to r_{++}$  are satisfied.

For the quantitative analysis of the motion, we employ an integration of the general equation of motion (2.20) in such way that we obtain two general equations for the trajectories described for the photons: unbounded and critical trajectories ( $0 < b \le b_c$ ) are described by Eq. (2.36) and are shown in Fig. 3, whereas orbits of the first and the second kind are described by Eq.(2.37), in which case the orbits are bounded.

As an application of our previous results, we obtain an exact expression in terms of the inverse  $\wp$ -Weierstraß function, for the deflection angle  $\widehat{\alpha}$  experienced by photons emitted with impact parameter  $b_d$  by a source with coordinates  $(r_{\bigstar}, \theta_{\bigstar})$  with respect to the black hole system (which acts as a gravitational lens). The photons are then received by an observer at  $(r_{\bigoplus}, -\theta_{\bigoplus})$  (see left top panel of Fig. 4). One important and interesting result is the physical type of the deflection experienced by the massless particles. Depending on the value of the impact parameters this can be either attractive or repulsive with respect to the black hole. This feature is better appreciated in the bottom left panel of Fig. 4, in which the deflection angle  $\widehat{\alpha}$  vanishes at a specific value of the impact parameter  $b_0$ .

#### Acknowledgments

This work was funded by the Comisión Nacional de Investigación Científica y Tecnológica through FONDECYT Grant No. 1181708 (GC), PAI Grant No. 79150053 (GC) and DOCTORADO Grant No. 21181476 (CO).

#### References

- [1] Weyl H 1917 Zur gravitationstheorie Annalen der Phys. 54 117.
- [2] Weyl H 1918 Reine infinitesimalgeometrie Math. Zeitschr. 2 384.
- [3] Weyl H 1918 Gravitation und electrizität Sitz. Ber. Preuss. Ak. Wiss. 465.
- [4] Bach R 1921 Zur Weylschen relativitätstheorie und der Weylschen erweiterung des krümmenstensorsbegriffs *Math. Zeitschr.* **9** 110.
- [5] Mišković O, Olea R and Tsoukalas M 2014 Renormalized AdS action and critical gravity J. High Energy Phys. 1408 108.
- [6] Riegart R J 1984 Birkhoff's theorem in conformal gravity Phys. Rev. Lett. 53 315.
- [7] Mennheim P D and Kazanas D 1989 Exact vacuum solution to conformal Weyl gravity and galactic rotation curves *Astrophys. J.* **342** 635.
- [8] Kazanas D and Mennheim P D 1991 General structure of the gravitational equations of motion in conformal Weyl gravity Astrophys. J. Suppl. **76** 431.
- [9] Mennheim P D and Kazanas D 1991 Solutions to the Reissner-Nordström, Kerr, and Kerr-Newman problems in fourth-order conformal Weyl gravity *Phys. Rev. D* 44 417.
- [10] Mennheim P D and Kazanas D 1994 Newtonian limit of conformal gravity and the lack of necessity of the second order Poisson equation Gen. Rel. Grav. 26 337.
- [11] Edery A and Paranjape M B 1998 Classical tests for Weyl gravity: Deflection of light and time delay *Phys. Rev. D* **58** 024011.
- [12] Pireaux S 2004 Light deflection in Weyl gravity: Critical distances for photon paths *Class. Quant. Grav.* **21** 1897.

- [13] Pireaux S 2004 Light deflection in Weyl gravity: Constraints on the linear parameter *Class. Quant. Grav.* **21** 4317.
- [14] Bhattacharya A, Panchenko A, Scalia M, Cattani C and Nandi K K 2010 Light bending in the galactic halo by Rindler–Ishak method *J. Cosmol. Astropart. Phys.* **1009** 004.
- [15] Sultana J and Kazanas D 2010 Bending of light in conformal Weyl gravity *Phys. Rev. D* 81 127502.
- [16] Sultana J, Kazanas D and Said J L 2012 Conformal Weyl gravity and perihelion precession Phys. Rev. D 86 084008.
- [17] Villanueva J R and Olivares M 2013 On the null trajectories in conformal Weyl gravity J. Cosmol. Astropart. Phys. 1306 040.
- [18] Finelli F, Galaverni M and Gruppuso A 2007 Light Bending as a Probe of the Nature of Dark Energy Phys. Rev. D 75 043003.
- [19] Said J L, Sultana J and Adami K Z 2013 Gravitomagnetic effects in conformal gravity Phys. Rev. D 88 087504.
- [20] Sultana J 2014 The Sagnac effect in conformal Weyl gravity Gen. Relativ. Gravit. 46 1710.
- [21] Mennheim P D and Kazanas D 1991 Solutions to the Reissner–Nordström, Kerr and Kerr-Newman problems in fourth-order conformal Weyl gravity *Phys. Rev. D* 44 417.
- [22] Klemm D 1998 Topological black holes in Weyl conformal gravity Class. Quantum Grav. 15 3195.
- [23] Said J L, Sultana J and Adami K Z 2012 Exact static cylindrical solution to conformal Weyl gravity Phys. Rev. D 85 104054.
- [24] Lu H, Pang Y, Pope C N and Vázquez–Poritz J F 2012 AdS and Lifshitz black holes in conformal and Einstein–Weyl gravities *Phys. Rev. D* 86 044011.
- [25] Payandeh F and Fathi M 2012 Spherical solutions due to the exterior geometry of a charged Weyl black hole *Int. J. Theor. Phys.* **51** 2227.
- [26] Lobo F S N 2008 General class of wormhole geometries in conformal Weyl gravity *Class. Quantum Grav.* **25** 175006.
- [27] Knox L and Kosowsky A 1993 Primordial nucleosynthesis in conformal Weyl gravity arXiv: 9311006
- [28] Diaferio A, Ostorero L and Cardone V F  $\gamma$ -ray bursts as cosmological probes:  $\Lambda$ CDM vs. conformal gravity *J. Cosmol. Astropart. Phys.* **1110** 008.
- [29] Diaferio A and Ostorero L 2009 X-ray clusters of galaxies in conformal gravity Mon. Not. Roy. Astron. Soc. **393** 215.
- [30] Mannheim P D 2012 Cosmological perturbations in conformal gravity Phys. Rev. D 85 124008.
- [31] Varieschi G U 2010 A kinematical approach to conformal cosmology Gen. Rel. Grav. 42 929.
- [32] Brihaye Y and Verbin Y 2009 Spherical structures in conformal gravity and its scalar–tensor extension Phys. Rev. D 80 124048.
- [33] Barabash O V and Pyatkovska H P 2008 Weak-field limit of conformal Weyl gravity Ukr. J. Phys. 53 737.
- [34] Villanueva J R, Tapia F, Molina M and Olivares M 2018 Null paths on a toroidal topological black hole in conformal Weyl gravity arXiv: 1808.04298
- [35] Chandrasekhar S 1983 The Mathematical Theory of Black Holes (New York: Oxford University Press.)

- [36] Cruz N, Olivares M and Villanueva J R 2005 The geodesic structure of the Schwarzschild anti-de Sitter Black Hole Class. Quant. Grav. 22 1167.
- [37] Shutz B 1990 A First Course in General Relativity (Cambridge: Cambridge University Press.)
- [38] Olivares M, Saavedra J, Leiva C and Villanueva J R 2011 Motion of charged particles on the Reissner-Nordström (Anti)—de Sitter black holes *Mod. Phys. Lett. A* 26 2923.
- [39] Jaklitsch M J, Hellaby C and Matravers D R 1989 Particle motion in the spherically symmetric vacuum solution with positive cosmological constant *Gen. Rel. Grav.* 21 941.
- [40] Villanueva J R, Saavedra J, Olivares M and Cruz N 2013 Photons motion in charged anti–de Sitter black holes Astrophys. Space Sci. **344** 437.
- [41] Halilsoy M, Gurtug O and Habib Mazharimousavi S 2013 Rindler modified Schwarzschild geodesics Gen. Rel. Grav. 45 2363.
- [42] Leiva C, Saavedra J and Villanueva J R 2009 The geodesic structure of the Schwarzschild black holes in gravity's Rainbow *Mod. Phys. Lett. A* 24 1443.
- [43] Wald R 1984 General Relativity (Chicago: University of Chicago Press.)
- [44] Balazs N L and Voros A 1986 Chaos on the pseudosphere Phys. Rept. 143 109.
- [45] Lightman A P, Press W H, Price R H and Teukolsky S A 1975 Problem Book in Relativity and Gravitation (New Jersey: Princeton University Press.)
- [46] Rindler W and Ishak M 2007 Contribution of the cosmological constant to the relativistic bending of light revisited *Phys. Rev. D* **76** 043006.
- [47] Ishak M and Rindler W 2010 The relevance of the cosmological constant for lensing *Gen. Rel. Grav.* 42 2247.
- [48] Ishak M, Rindler W and Dossett J 2010 More on lensing by a cosmological constant *Mon. Not. Roy. Astron. Soc.* **403** 2152.
- [49] Byrd P F and Friedman M D 1971 Handbook of Elliptic Integrals for Engineers and Scientists (Berlin: Springer-Verlag)
- [50] Hancock H 1958 Lectures on the theory of elliptic functions (New York: Dover publications Inc.)
- [51] Armitage J V and Eberlein W F 2006 Elliptic functions, London Mathematical Society Student Texts. (No. 67) (Cambridge: Cambridge University Press.)
- [52] Gradshteyn I S and Ryzhik I M 2007 Table of integrals, series, and products (London: Academic Press.)